Adv. Radio Sci., 6, 39–44, 2008
www.adv-radio-sci.net/6/39/2008/

Advances in Radio Science

Sievenpiper HIS and its influence on antenna correlation

S. K. Hampel, O. Schmitz, and I. Rolfes

Leibniz Universität Hannover, Institut für Hochfrequenztechnik und Funksysteme, Appelstr. 9A, 30167 Hannover, Germany

Abstract. This paper deals with the influence of artificial magnetic conductors (AMC), so-called Sievenpiper High Impedance Surfaces (HIS), on the MIMO and Diversity performance of a planar linear-polarized 2×2 dipole array in the ISM-band at 2.45 GHz. The characteristic performance criteria such as envelope correlation coefficient, spectral efficiency, Mean Effective Gain (MEG) and Diversity gain of a coupled 2×2 dipole array are investigated. By means of full-wave electromagnetic analysis as well as Monte-Carlo simulations applying statistical channel models the characteristic antenna pattern just as the MIMO and Diversity analysis is performed, respectively. The obtained results show that the application of Sievenpiper High Impedance Surfaces to planar antenna arrays enables good MIMO and Diversity performance compared to ideal configurations in free-space while offering the design of low profile antennas with simultaneously enhanced characteristics.

1 Introduction

With nowadays wireless communication techniques and the upcoming new standards like IEEE 802.11n (MIMO WLAN), UWB or LTE it is obvious that a huge demand for higher data rates still exists. Concerning Edholm's Law the border of data transmission with 1 Gbit/s will be reached in the near future. On the one hand modulation schemes and coding algorithms in the classical way cannot achieve much more spectral efficiency. On the other hand bandwidth as well as transmit power are regulated. Consequently new concepts in terms of MIMO and Diversity have to be investigated in order to reach the goal of high data rates and reliable transmission links.

Correspondence to: S. K. Hampel
(hampel@hft.uni-hannover.de)

Furthermore, Moores Law indicates higher integration levels with enhanced transistor technology. This in turn paves the way for increasing functionality with constant chip area consumption or decreasing die sizes while keeping functionality constant.

These two aspects for performance enhancement of wireless communication systems call for appropriate low profile antenna designs with MIMO and Diversity capability. Therefore, this paper deals with the impact of so-called Sievenpiper HIS (see Sievenpiper, 1999) on antenna correlation, which is a critical factor when considering the MIMO and Diversity performance of multi-element-antenna setups (MEA). The Sievenpiper HIS themselves exhibit the possibility of designing low profile antennas with high efficiency while using constructive interference mechanisms based on the characteristic behavior of so-called artificial magnetic conductors (AMC). Furthermore the shielding effect of this spatial filter prevents electromagnetic interactions with biological systems (user) or circuitry in the handheld. This eases the perturbation occuring in the communication terminal while conserving the radiation efficiency of the antenna as well as shielding the environment against unwanted radiation.

Therefore the main goal is to investigate the influence of these HIS on the correlation properties affected by the antenna coupling as well as the consequences considering the spectral efficiency of a 2×2 MIMO system and its Diversity gain and Mean Effective Gain (MEG) mainly controlled by the gain pattern of the antenna setup.

The organization of the paper is as follows. In Sect. 2 a brief description of the underlying theory concerning Sievenpiper HIS is presented. Sections 3 and 4 introduce the Diversity and MIMO analysis with its characteristics in general terms. Initial and detailed results regarding the antenna characterization as well as Diversity and MIMO performance based on stochastic envelope processes for the spatial profile of the incident and radiated waves at the receive and the

Published by Copernicus Publications on behalf of the URSI Landesausschuss in der Bundesrepublik Deutschland e.V.

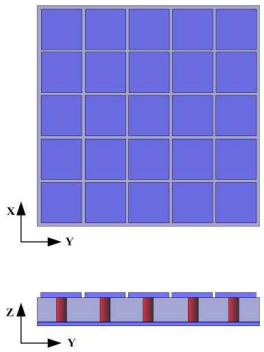

Fig. 1. Top and side view of a Sievenpiper HIS with square patches placed in the xy-plane.

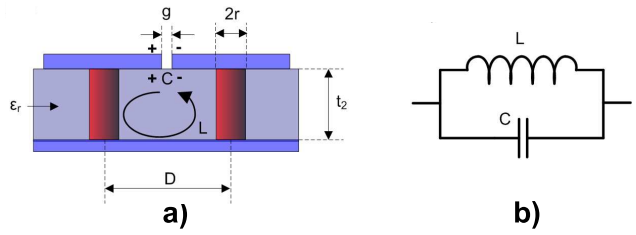

Fig. 2. (a) Side view of two unit cells. **(b)** Equivalent parallel resonant circuit.

transmitter are given in Sect. 5.

2 Basics of Sievenpiper HIS

The Sievenpiper HIS can be regarded as composite material consisting of a frequency selective surface (FSS) on a conducter backed dielectric substrate with periodically embedded cylindrical vias as shown in Fig. 1.

Its underlying theory is in general based on the effective medium theory (see Merill, 1999) and moreover on the transmission line theory. Assuming that the physical sizes of all geometry parameters are much smaller than the effective wavelength corresponding to the frequency of operation, i.e. $t_2, r, D, g \ll \lambda_{\text{eff}}$ (see Fig. 2a), a description of the electromagnetic properties of the Sievenpiper HIS by the use of the above mentioned transmission line theory is applicable. Therefore, only a fraction of the whole structure, a so-called unit cell (see Fig. 2a), is sufficient to describe the behavior of the complete periodic two dimensional filter with the periodicity D. The metallic FSS on top of the grounded dielectric host substrate with permittivity ϵ_r forms a parallel resonant circuit as depicted in Fig. 2b. Here the capacitive part of the surface impedance is provided by the FSS grid whereas the inductive surface impedance is a property of the substrate (see Clavijo, 2003). The effective capacitance C_{FSS} and effective inductance L_{Sub} forming the parallel resonant circuit can be expressed as follows:

$$C_{\text{FSS}} = \epsilon_{\text{eff}}\epsilon_0 \frac{2D}{\pi} \ln\left(\frac{2D}{\pi g}\right) \qquad (1)$$

$$L_{\text{Sub}} = \mu_0 \mu_r t_2$$

For simplicity in a first approximation polarization as well as angular dependency are dropped. From Eq. (1) it can be obtained that the reactive characteristics of the FSS layer and the host substrate are mainly related to the gap-width g, the periodicity D, the effective dielectric constant ϵ_{eff} and the substrate height t_2, respectively. At resonant frequency of the resulting parallel resonant circuit, $\omega_0 = 1/\sqrt{L_{\text{Sub}} C_{\text{FSS}}}$, the extremely high surface impedance of the structure leads to a vanishing magnetic field (AMC). This yields to a reflection coefficient with a magnitude of $\Gamma = 1$ and a phase of $\phi_\Gamma = 0°$. The operational bandwidth of the in-phase reflection is determined by the corner frequencies with $\phi_\Gamma = \pm\pi/2$. These borders arise from the assumption of a radiator placed infinitely close above the surface of the HIS. This will result in more constructive than destructive interference of a directly radiated and reflected wave in the upper hemisphere within these bounds.

The surface wave suppression phenomenom of the Sievenpiper HIS leading to electromagnetic band-gap structures (EBG) will be omitted here. For the interested reader we refer to Clavijo (2003) and Goussetis (2006) for more information about the EBG behavior of the Sievenpiper HIS.

3 Diversity analysis

The intention of applying Diversity with multiple receive and/or transmit antennas in wireless communication systems is to overcome the drawbacks like fading and depolarisation comprising the signal transmitted over the wireless channel (see Jakes, 1974). Therefore different Diversity techniques like spatial-, pattern- or polarization-Diversity can be implemented in a transceiver to reduce these signal impairments with the benefit of either increasing the transmission link reliability or the effective data rate both by increasing the available SNR at the receiver. An important characteristic influencing the Diversity performance is the complex correlation coefficient of incoming signals resulting from signal correlation within the channel and the antenna correlation between each element of a MEA system. The correlation influences the achievable Diversity gain, which is a measure for the reduction of the channel imposed data link impairments. The complex correlation coefficient between antenna element i and j of a receiver is given in Eq. (2). Here R and σ represent the covariance term and the standard deviation, respectively.

$$\rho_{i,j} = \frac{R_{i,j}}{\sqrt{\sigma_i^2 \sigma_j^2}}, \qquad (2)$$

The definition of the covariance $R_{i,j}$ in Eq. (2) is given by Fujimoto (2001) and shown in Eq. (3).In this expression

$C_{\vartheta_i,\varphi_i}(\vartheta,\varphi)$ denotes the far field pattern of the specific antenna i and j, respectively, decomposed into its two polarization components in elevation ϑ and azimuth φ corresponding to a spherical coordinate system. Moreover * indicates the conjugate complex, $\boldsymbol{k}$ is the wavevector and r_{ij} is the distance between the indicated antenna elements. XPR is called cross polarization ratio and is a channel property which indicates the conversion of a linear-polarized radiated wave in its corresponding orthogonal component. The two dimensional probability distribution $p_{\vartheta,\varphi(\vartheta,\varphi)}$ is corresponding to the anlge of arrival (AOA) and angle of departure (AOD) behaviour of the incoming and radiated waves, respectively, in a statistical channel model scenario. Here AOA and AOD are given by a Laplacian distribution in azimuth and a Gaussian distribution in elevation (see Waldschmidt, 2004).

$$\begin{aligned} \mathrm{R_{i,j}} = \int_0^{2\pi}\int_0^{\pi} \Big[& C_{\vartheta_i}(\vartheta,\varphi)\cdot C^*_{\vartheta_j}(\vartheta,\varphi) + \cdots \\ & \cdots + \mathrm{XPR}\cdot C_{\varphi_i}(\vartheta,\varphi)\cdot C^*_{\varphi_j}(\vartheta,\varphi)\Big] \times \cdots \\ & \cdots \times p_{\vartheta,\varphi}(\vartheta,\varphi)\cdot e^{\mathrm{j}\mathrm{kr_{ij}}\sin(\vartheta)} d\vartheta\, d\varphi \ . \end{aligned} \tag{3}$$

In case of a fading environment with Rayleigh distributed signal envelope and equally distributed signal phase the so-called envelope correlation $\rho_{\mathrm{e_{i,j}}}$ can be approximated by

$$\rho_{e_{i,j}} \approx \left|\rho_{i,j}\right|^2 . \tag{4}$$

Furthermore the characteristic known as MEG, which denotes the ratio of the mean received power to the mean incident power of an antenna, is the second figure of merrit while evaluating Diversity performance of MEA systems. The MEG can be expressed as (see Fujimoto, 2001)

$$\begin{aligned} \mathrm{MEG}_i = \int_0^{2\pi}\int_0^{\pi} \Bigg[& \frac{\mathrm{XPR}}{1+\mathrm{XPR}} G_{\vartheta,i}(\vartheta,\varphi) + \cdots \\ & \frac{1}{1+\mathrm{XPR}} G_{\varphi,i}(\vartheta,\varphi)\Bigg] p_{\vartheta,\varphi}(\vartheta,\varphi)\sin(\vartheta)\, d\vartheta\, d\varphi, \end{aligned} \tag{5}$$

with $G_{\vartheta,\varphi_i(\vartheta,\varphi)}$ the absolute antenna gain pattern in azimuth and elevation of element i.

4 MIMO analysis

Similar to Diversity techniques MIMO systems try to take advantage of the multipath propagation properties of wireless communication channels. Here parallel transmission of data streams over M transmit antennas should lead to a boost in data rate while exploiting the spatio-temporal properties of the channel by an MEA arrangement. The use of N receive antennas leads to a $M\times N$ channel matrix $\mathbf{H}$ with complex coefficients h_{mn} (Rayleigh distributed amplitude and equally distributed phase), mapping the M transmitted signals of the transmit vector $\boldsymbol{x}$ on N received signals of the receive vector $\boldsymbol{y}$, as stated in Eq. (6). The reduction of the $M\cdot N$ channel impulse responses to simple complex coefficients is valid as long as the channel is assumed to be narrowband (see Tse, 2004).

$$\begin{pmatrix} y_1 \\ y_2 \\ \vdots \\ y_m \end{pmatrix} = \begin{pmatrix} h_{11} & h_{12} & \dots & h_{1n} \\ h_{21} & h_{22} & \dots & h_{2n} \\ \vdots & \vdots & \ddots & \vdots \\ h_{m1} & h_{m2} & \cdots & h_{mn} \end{pmatrix} \cdot \begin{pmatrix} x_1 \\ x_2 \\ \vdots \\ x_n \end{pmatrix} \tag{6}$$

Expanding the well known Shannon formula for channel capacity C of a SISO system to MIMO channel capacity C_{MIMO} yields the following equation

$$\begin{aligned} C_{\mathrm{MIMO}} &= \log_2\ det\left(\bar{\mathbf{I}} - \frac{P_T}{M\sigma_n^2} H H^H\right) \\ C_{\mathrm{MIMO}} &= \sum_i \log_2\left(1 + \frac{P_T}{M\sigma_n^2}\lambda_i\right) \end{aligned} \tag{7}$$

Here $\mathbf{I}$ represents the identity matrix, P_T is the total transmit power equally allocated to the M transmit antennas, σ_n^2 is the noise power of the assumed white gaussian noise affecting the received signal, H^H represents the hermitian of the channel matrix $\mathbf{H}$ and λ_i is the i-th eigenvalue of the underlying eigenvalue problem. The maximum number of useable subchannels is limited to the maximum number of eigenvalues ($\min(M, N)$). The rank of the matrix and the strength of the eigenvalues λ_i as well as the number of useable subchannels depends on the signal correlation introduced in the former section. The higher the correlation the lower the distict subchannel capacity which results in a waste of transmit power allocated to this subchannel. Likewise to the afore presented Diversity analysis the success and benefit of MIMO transmission is bound to the strength of signal correlation, which means: low correlation leads to a maximum in performance, here MIMO channel capacity.

5 Simulation results

In this section a coupled MEA setup with HIS will be evaluated in comparison to its equivalent coupled free-space model (FS) with respect to its Diversity and MIMO performance. Based on full-wave electromagnetic simulation and Monte-Carlo analysis, the specific antenna characteristics, like input-matching and gain pattern as well as the antenna correlation, the Diversity gain, the MEG and the channel capacity will be presented, respectively.

5.1 Array setup and input matching

A picture of the investigated setup is shown in Fig. 3. A coupled 2×2 planar dipole array with element spacing d is placed Δh=4 mm above a customized HIS. The dipoles and HIS frequency of operation is defined to be f_0=2.45 GHz in FS. Therefore the distance between dipoles and HIS is approximately $\Delta h=\lambda_0/30$ with λ_0 being the corresponding wavelength to f_0. The input return loss and the resulting

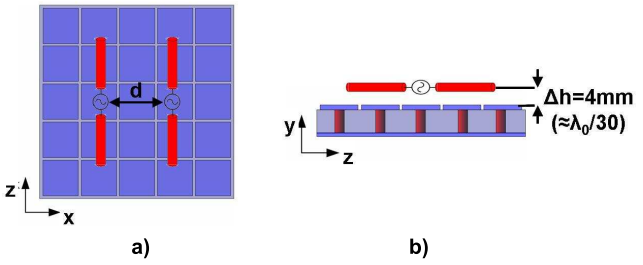

Fig. 3. **(a)** Top and **(b)** side view of the array configuration with HIS.

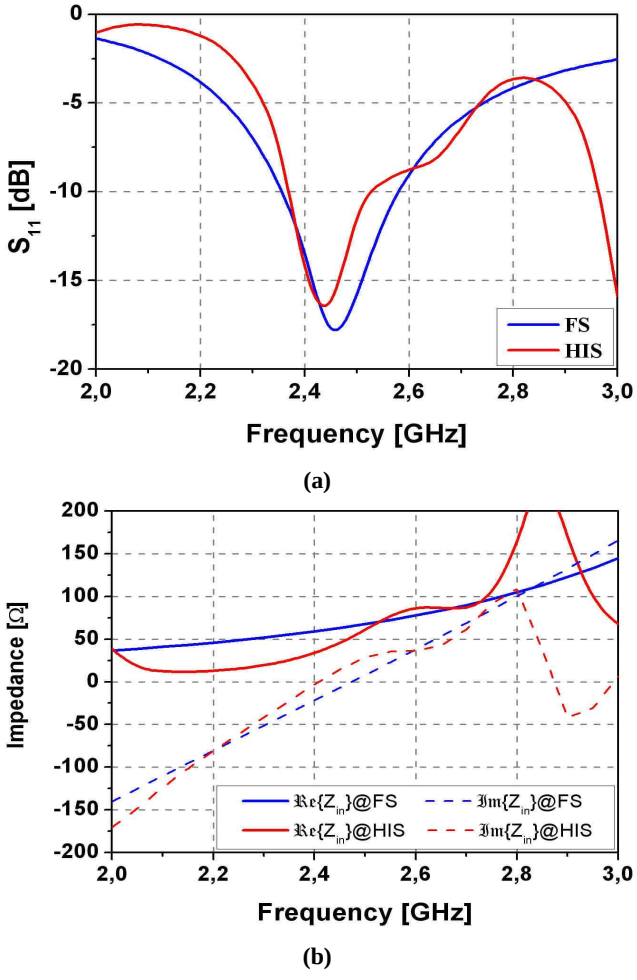

Fig. 4. Input matching **(a)** and resulting input impedance **(b)** over frequency of one dipole above HIS (red) and in FS (blue).

input impedance of one dipole is depicted in Fig. 4 and compared to an equivalent free-space dipole resonating at 2.45 GHz to underline the functionality of the HIS. For the HIS setup a good input match with a reflection coefficient S_{11} less then −15 dB and a purely real input impedance of $\mathrm{Re}\{Z_{in}\}\approx 40\,\Omega$ can be observed.

Table 1. Statistical parameter of applied channel scenarios.

	Statistical parameter			
	m_ϑ	σ_ϑ	m_φ	σ_φ
CS1	90°	10°	60°	20°
CS2	90°	10°	90°	20°

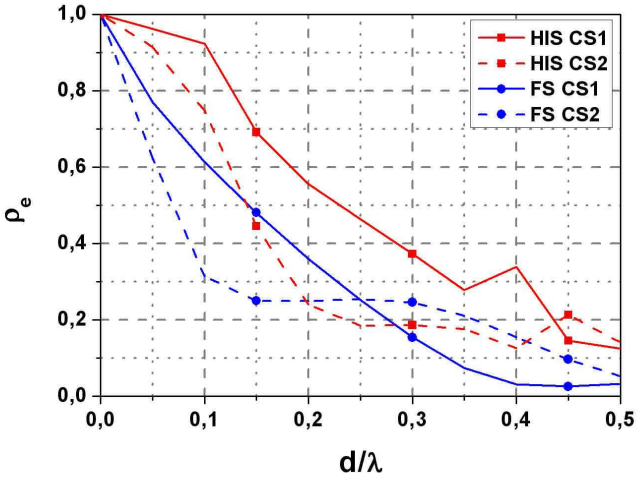

Fig. 5. Envelope correlation ρ_e over interelement spacing d of dipole array above HIS (red) and in FS (blue) for CS1 (solid) and CS2 (dashed).

5.2 Correlation properties and MIMO performance

Since an adequate functionality of the dipole in conjunction with the HIS is proven, the antenna correlation of both setups will be investigated while varying the interelement spacing d between both antennas from d=0 to d=$\lambda/2$. Furthermore two different channel scenarios (CS) will be used during the Monte Carlo simulation with the statistical parameters in Table 1 while the XPR was kept constant with 0 dB. Figure 5 shows the resulting curves for the envelope correlation over d in both CS for both arrangements while the SNR in Eq. (7) was set to 20 dB. It can be seen that, with increasing interelement spacing, the correlation relaxes. Furthermore the correlation for CS2 in main beam direction reveals a decrease in correlation as well (for HIS and FS). This behaviour is well known in literature and was expected due to the decorrelating influence of the exponential term in Eq. (3). Moreover, the setup with HIS offers higher correlation than the FS array except for the case of $d/\lambda \geq$=0.25 in CS2. The higher correlation of the HIS setup in contrast to the FS arrangement can be explained while considering the radiation pattern for a fixed spacing (here d/λ=0.25) shown in Fig. 6. As can be seen by the red lined pattern the constructive interference due to the reflection of the radiated wave on the HIS surface leads to a loss in pattern Diversity with respect to the FS pattern. Here

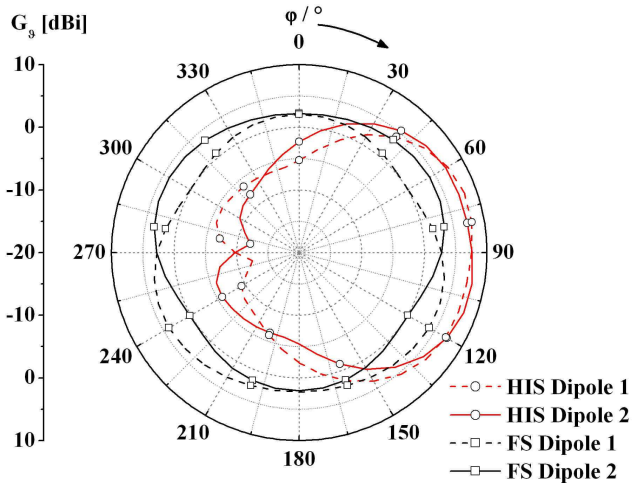

Fig. 6. Gain pattern for interelement spacing d=λ/4 for each dipole of both dipole array arrangements: HIS (red) and FS (black).

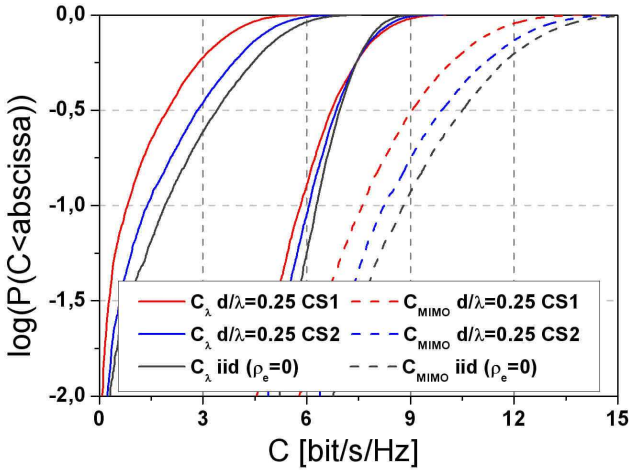

Fig. 7. CDF of subchannel capacity (C_λ) and total capacity (C_{MIMO}) for the dipole array with HIS for d=λ/4 in CS1 (red) and CS2 (blue) compared with uncorrelated Rayleigh process (iid, grey).

Table 2. Envelope correlation and 10%-outage capacity for the dipole array with HIS for d=λ/4 in CS1&CS2 compared to an uncorrelated Rayleigh process iid.

	ρ_e	$C_{10\%\mathrm{out}}$ [bit/s/Hz]	% of $C_{10\%out,max}$
CS1	0.46	7.61	86.5
CS2	0.18	8.24	98.4
iid	0	8.8	100

Table 3. MEG and MEG-ratio for both dipoles in both arrangements for d=λ/4 and CS1.

	MEG_1 [dBi]	MEG_2 [dBi]	$\mathrm{R}_{\mathrm{MEG}}$ [dB]
HIS	3.35	3.55	0.2
FS	0.46	−2.4	2.86

the difference in the shape of the two radiating antennas is more distinct which yields to less correlation. Furthermore, the differences in pattern shape over the azimuth angle φ in the case of the FS array results in less sensitivity to a change in mean of AOA.

The estimated MIMO channel capacity in terms of the cumulative distributed function (CDF) and the so-called 10%-outage capacity $\mathrm{C}_{10\%\mathrm{out}}$ for d/λ=0.25 in both CS is given in Fig. 7 and Table 2, respectively. Here only the dipoles with HIS filter are considered due to the fact that the results for the FS array offer approximately the same correlation in both CS as the HIS arrangement for CS2. Furthermore, the Rayleigh-curve for identically independently distributed (iid) channel coefficients without any correlation is given, which can be regarded as the maximum achievable capacity for a 2×2 array.

The CDF can be interpreted as probability of the capacity to be higher than the corresponding abscissa value. The analysis of these results reveals the expected worse performance of the HIS setup due to higher correlation. Nevertheless, these results are not as bad as it seems, taking into account that only normalized patterns ($C_{\vartheta,\varphi,i(\vartheta,\varphi)}$) have been used for the estimation of the correlation coefficient and the enhanced antenna gain and the associated benefits were dropped during this analysis. This aspect will be investigated in the next subsection dealing with the achieveable Diversity performance. Due to this lack of gain performance, values of $C_{10\%\mathrm{out}}\geq$86% of $C_{10\%\mathrm{out,max}}$ can be considered as adequate result.

5.3 Diversity performance

For the purpose of comparison and conclusiveness the following results dealing with the Diversity performance of the dipole array were carried out for the same antenna spacing as for the channel capacity in the preceding subsection, d/λ=0.25. Furthermore, the analysis is limited to CS1 where the poor MIMO performance was realized, while here Diversity offers a promising alternative for performance enhancement of a supposed data transmission link. This is straightforward because of the afore mentioned discrepancy of dropping the absolute gain value while processing the MIMO capacity. The results for the distinct MEG of each antenna as well as the MEG-ratio, based on the gain pattern depicted in Fig. 6 with a maximum gain in main beam direction of the distinct arrangements of $G_{i,\mathrm{HIS}}$=8 dB and $G_{i,\mathrm{FS}}$=4 dB for HIS and FS, respectively, are summarized in Table 3.

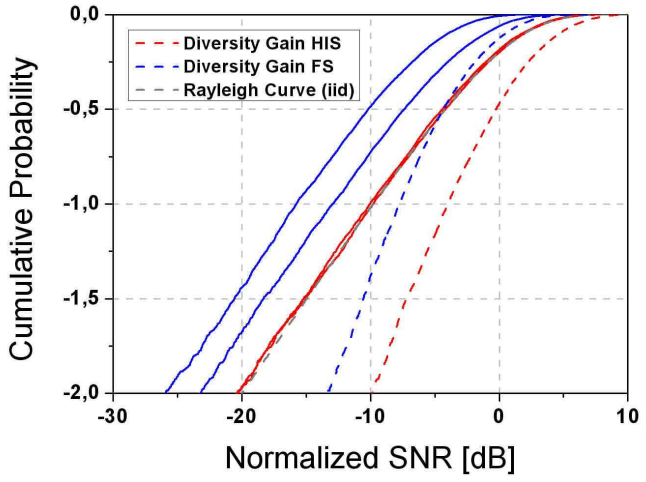

Fig. 8. CDF of available SNR for both dipole arrays, HIS (red) and FS (blue), for $d=\lambda/4$ in CS1 compared to an uncorrelated Rayleigh process (iid, grey).

Due to the higher gain of the MEA setup in conjunction with the HIS in the proposed primary radiation hemisphere ($0°\leq\varphi\leq180°$) compared to the FS array, the increase of the MEG of about 3 dB and 6 dB is obvious keeping in mind the depency of the MEG on the antenna gain (see Eq. 5).

A variation of the XPR is not appropriate within this investigation, due to the fact, that the power imbalance is only interesting in case of polarization Diversity, which is not applicable when using two parallel oriented linearly polarized antennas with vanishing cross-polarized component. In Fig. 8 the CDF of the normalized SNR is depicted applying maximum ratio combining as Diversity technique. It can be seen that both arrangements achieve a good performance concerning the Diversity gain with G_{HIS}=5.88 dB and G_{HIS}=7.86 dB for the HIS and FS configuration, respectively, in case of a given outage probability level of 1%. More important is the additional shift in available SNR of approximately 4 dB when applying the HIS. This can be ascribed to the increased MEG. This consequently leads to the conclusion that the dipole array with HIS performs better compared to the reference FS setup in case of spatial directivity of the wireless channel even though the envelope correlation is higher.

6 Conclusions

In this article the influence of Sievenpiper HIS on the correlation properties of a 2×2 array consisting of planar dipoles was investigated. The obtained results concerning envelope correlation over interelement spacing, MIMO channel capacity, MEG and Diversity gain have been compared to a reference array in FS. Here two different spatial channel scenarios of incident waves, CS1 and CS2, were regarded to evaluate the array performance. Although the correlation properties of the dipoles in conjunction with the HIS were not as good as the correlation of the FS setup, the MIMO capacity reveals good results anyhow. Furthermore the Diverstity performance of the HIS setup, given by the MEG and the Diversity gain, outperforms the FS array due to a huge increase in antenna gain based on constructive interference of radiated and reflected waves. Therefore when considering MIMO and Diversity systems the use of conventional and well known planar antenna concepts in conjunction with Sievenpiper HIS is applicable. In addition to the enhanced antenna performance the HIS offers the possibility of designing planar low profile antennas with small geometrical dimensions for integration in wireless transmission terminals instead of conventional planar conductor backed or external vertical monopole antennas.

References

Clavijo, S.: Design Methodology for Sievenpiper High-Impedance Surfaces: An Artificial Magnetic Conductor for Positive Gain Electrically Small Antennas, IEEE Trans. Antennas and Propagation, 51, 2678–2690, 2003.

Fujimoto, K.: Mobile Antenna Systems Handbook, Artech House, Boston, 2001.

Goussetis, G.: Tailoring the AMC and EBG characteristics of periodic metallic arrays printed on grounded dielectric substrate, IEEE Trans. Antennas and Propagation, 54, 82–89, 2006.

Jakes, W. C.: Microwave Mobile Communications, IEEE Press. Inc., New York, 1974.

Merill, W. M.: Effective Medium Theories for Artificial Materials Composed of Multiple Sizes of Spherical Inclusions in a Host Continuum, IEEE Trans. Antennas and Propagation, 47, 142–148, 1999.

Sievenpiper, D. F.: High-Impedance Electromagnetic Surfaces, Dissertation, University of California, Los Angeles, 1999.

Tse, D.: Fundamentals of Wireless Communications, University of California, Berkeley, 2004.

Waldschmidt, C.: Compact Wide-Band Multimode Antennas for MIMO and Diversity, IEEE Trans. Antennas and Propagation, 52, 1963–1969, 2004.